2016-06-01

Modification of the In Vitro Uptake Mechanism and Anti-Oxidant Levels in HaCaT Cells and Resultant Changes to Toxicity and Oxidative Stress of G4 and G6 Poly (amido amine) Dendrimer Nanoparticles.

Marcus Maher
Technological University Dublin

Hugh Byrne
Technological University Dublin, hugh.byrne@tudublin.ie

Recommended Citation
Maher, M. and Byrne, H., (2016) Modification of the in vitro uptake mechanism and anti-oxidant levels in HaCaT cells and resultant changes to toxicity and oxidative stress of G4 and G6 Poly (amido amine) dendrimer nanoparticles. *Analytical and Bioanalytical Chemistry*, 408, 5295-5307 (2016)

Funder: DIT

Modification of the *in vitro* uptake mechanism and anti-oxidant levels in HaCaT cells and resultant changes to toxicity and oxidative stress of G4 and G6 Poly (amido amine) dendrimer nanoparticles.

Marcus A. Maher[1,2,*], Hugh J. Byrne[1]

[1]FOCAS Research Institute, Dublin Institute of Technology, Kevin Street, Dublin 8, Ireland

[2]School of Physics, Dublin Institute of Technology, Kevin Street, Dublin 8, Ireland

*Corresponding author: marcus.maher@mydit.ie

Keywords:

Dendrimer nanoparticles

PAMAM nanoparticles

Endocytosis

Passive diffusion

Oxidative stress

Membrane permeability

Abstract:

The mechanism of cellular uptake by endocytosis and subsequent oxidative stress has been identified as the paradigm for the toxic response of cationically surface charged nanoparticles. In an attempt to circumvent the process, the effect of increased cellular membrane permeability on the uptake mechanisms of poly (amidoamine) dendrimers generation 4 (G4) and 6 (G6) *in vitro* was investigated. Immortalised, non-cancerous human keratinocyte (HaCaT) cells were treated with DL-Buthionine-(S,R)-sulfoximine (BSO). Active uptake of the particles was monitored using fluorescence microscopy to identify and quantify endosomal activity and resultant oxidative stress, manifest as increased levels of reactive oxygen species, monitored using the carboxy-H_2DCFDA dye. Dose dependent cytotoxicity for G4 and G6 exposure was registered using the cytotoxicity assays Alamar Blue and MTT, from 6 to 72 hours.

Reduced uptake by endocytosis is observed for both dendrimer species. A dramatic change, compared to untreated cells, is observed in the cytotoxic and oxidative stress response of the BSO treated cells. The significantly increased mitochondrial activity, dose dependent anti-oxidant behaviour and reduced degree of endocytosis for both dendrimer generations, in BSO treated cells, indicates enhanced permeability of the cell membrane, resulting in the passive, diffusive uptake of dendrimers, replacing endocytosis as the primary uptake mechanism. The complex MTT response reflects the importance of glutathione in maintaining redox balance within the mitochondria. The study highlights the importance of regulation of this redox balance for cell metabolism, but also points to the potential of controlling the nanoparticle uptake mechanisms, and resultant cytotoxicity, with implications for nanomedicine.

Introduction

Nanoparticle science is a rapidly advancing field which holds much promise in areas such as targeted drug and gene delivery.[1,2,3] However, nanoparticle uptake into a cell has been demonstrated, particularly for nanoparticles with an effective cationic surface charge, to give rise to cytotoxic responses, raising concerns about the potential health and environmental impact of the proliferation of nanomaterials in consumer products.[4] A systematic understanding of the mechanisms of toxicity and their dependence on nanoparticle physico-chemical properties on a cellular level is therefore required.[5] In the context of nanomedical applications, understanding and controlling the uptake process and subcellular trafficking of the delivery vehicle and the bioavailability of the cargo are critically important.

Cellular uptake of nanoparticles principally occurs via endocytosis, whereby the nanoparticle is invaginated by the cellular membrane and is transported into the cell.[6] As the low pH environment of the endosome attempts to digest the nanoparticle, the redox balance of the cell is disrupted, and, in the case of nanoparticles with an effective cationic surface charge, the process gives rise to an increase in the production of Reactive Oxygen Species (ROS), localised mainly around the endosome (or later lysosome).[6,7,8,9] Although intra cellular anti-oxidants attempt to neutralise the imbalance, ROS production can be sufficient to lead to oxidative stress.[10] Subsequently, a cascade of events and the release of several characteristic cytokines and chemokines occurs, ultimately leading to cell death, a process which is the accepted paradigm of nanotoxicity of many nanoparticles *in vitro*.[6] The process has been well demonstrated for model nanoparticle system such as amine functionalised polystyrene,[11,12,13] amorphous nanosilica,[14] and nanomeric polymeric dendrimers.[10]

Aminated molecules are intrinsic antioxidants, however, and generally regarded as ROS scavengers. As examples, spermine and spermidine have both been shown to reduce Fe^{3+} to Fe^{2+} [15] and the ferric reducing activity of these molecules has been identified as a measure of anti-oxidant potential.[16] Carnosine, an endogenous dipeptide, has been shown to scavenge both reactive oxygen and nitrogen species.[17] Notably, in a study by Khalid *et al.* (*2015*), while the larger, higher generations of the aminated nanoscale dendrimers Poly (propylene imine) (PPI) were demonstrated to elicit oxidative stress and significant toxicity, the smaller, lower generations exhibited intracellular antioxidant behaviour and low toxicity.[18] Examination of the uptake mechanisms indicated a transition from cellular uptake by passive diffusion at low generations to active endocytosis for higher generations. The study suggests that, in the case of catatonically charge nanoparticles, the endocytotic uptake and trafficking process is, in itself, a source of cellular toxicity. In the context of drug delivery, invagination of the delivery vehicle and cargo in this harsh environment may also be undesirable, and although escape by endosomolysis is a potential strategy,[19] this too can be a harsh process, causing significant damage to the cell.[20,21] For these reasons, circumventing endocytosis appears to be a valid strategy for the reduction of toxicity associated with aminated nanoparticles as well as nanoparticle drug or gene delivery.

Guarnieri *et al.* (*2015*), demonstrated that functionalization of aminated polystyrene nanoparticles with the viral peptide gH625 (derived from *Herpes simplex virus – 1*), which has a membrane perturbing domain, enables translocation of particles to the cytoplasm, avoiding endocytosis and thus, dramatically reducing the cytotoxicity.[22] An alternative strategy to increase

the permeability of the cellular membrane, *in vitro*, is through the application of DL-Buthionine-(*S*,*R*)-sulfoximine (BSO). BSO has previously been employed to study the effects of the reduction of levels of the intracellular antioxidant glutathione (GSH); and therefore oxidative stress[23,24,25,26] and has been shown to cause membrane permeabilisation.[27,28] BSO works as an inhibitor of the enzyme Glutamate Cysteine Ligase (EC 6.3.2.2) (historically known as gamma-glutamylcysteine synthetase) which is the first step in the production of GSH in the cell.[29] This reduction in GSH causes several different effects, one being the induction of the membrane permeability transition in the mitochondria.[30,31,32] The opening of this pore and the depletion of GSH allows ROS to diffuse from the mitochondria to the cell and via lipid peroxidation, cause damage to the cell membrane,[28] leading to increased permeability.

The reduction of GSH in the cell can have other adverse effects, however, mainly due to the fact that GSH is one of the main antioxidants involved in maintaining the redox balance of the mitochondria.[33] In the mitochondria, endogenous ROS is produced as a by-product of normal metabolism and therefore completely eliminating GSH can leave the cell susceptible to damage from this ROS.[34] Furthermore, reductions in cellular GSH can also lead to changes in the regulation of Ca^{2+} distribution[35,36,37] and the activation/deactivation of signalling pathways involved with growth, differentiation and apoptosis.[33,38,39,40] The loss of GSH and subsequent changes in the cell have been implicated in several disease states which is reviewed elsewhere.[34]

This study explores the impact, for HaCaT cell, of BSO treatment on the cellular uptake of, and subsequent oxidative stress and toxic response to, poly (amido amine) (PAMAM) dendrimers. These nanoscale aminated dendrimers have a systematically variable molecular structure, and the

homologous series of increasing generation, and concomitant size and number of surface amino groups, has been demonstrated to be ideal to study the dependence of nanoparticle cellular interactions on the physico-chemical properties of the particles. Previous studies have examined the structurally dependent toxicity, and underlying mechanisms of endocytosis, oxidative stress, immune responses and consequent toxicity[7,8,9,10] and the responses have been numerically modelled, as a guide towards a predictive toxicology approach.[10,41] For consistency and to allow comparisons with the previous work, the *in vitro* studies reported here were also carried out using the immortalised human keratinocyte cell line, HaCaT, and identical oxidative stress and cytotoxic assays. Furthermore, PAMAM dendrimers of Generation 4 and 6 were chosen as the extremes of the previously reported cytotoxicological response. In comparison, it is demonstrated that treatment with BSO results in a significant change in the nanoparticle uptake mechanisms and cytotoxicity.

Materials and Methods

Materials

DMEM F12 HAM growth medium, Penicillin, Streptomycin, fluorescently labelled, Polystyrene nanoparticles, with amine surface modification (PSNP-NH_2) 100nm, DL-Buthionine-(*S,R*)-sulfoximine(BSO) and 3-(4,5-dimethylthiazol-2-yl)-2,5-diphenyltetrazolium bromide (MTT) dye were purchased from Sigma-Aldrich, Ireland. The PAMAM dendrimer nanoparticles, generations 4 (molecular weight: 14,214 g/mol) and 6 (molecular weight: 58,046 g/mol), were purchased from Sigma-Aldrich and manufactured by Dendritech Inc. ThiolTracker™ Violet (TTV), CellLight® Early Endosomes-RFP, BacMam 2.0, Fetal Bovine Serum (FBS), L-Glutamine, Alamar Blue (AB) and 5-(and-6)-carboxy-2',7'-dichlorodihydrofluorescein diacetate (carboxy-H_2DCFDA) dye were purchased from Life Technologies™, Bio-Sciences, Ireland. HaCaT cells were purchased from Cell Line Services (CLS), Eppelheim, Germany. TrueLine 96-well cell culture plates were used for all viability and ROS studies.

All fluorescence and absorbance readings were taken on a Molecular Devices SpectraMax M3 Spectrometer. Confocal Laser Scanning Fluorescence Microscopy (CLSM) images were taken on a Zeiss LSM 510 Confocal Laser Scanning Microscope and processed using ImageJ software (with co-localisation analysis performed with the JaCoP plugin for ImageJ). All viability, ROS and GSH data analysis was performed using SigmaPlot v10.0 software.

Methods

Cell culture

HaCaT cells are an immortalised, non cancerous human keratinocyte cell line and were used for

these experiments. The cells were cultured in DMEM F12 HAM supplemented with 10% FBS, 45 IU/mL penicillin, 45 IU/mL streptomycin and 2mM L-glutamine at 37˚C in 5% CO_2. All assays carried out in this set of experiments were performed in 96 well plates, with cells plated at a concentration of $1x10^4$ cells/well in 100µL of DMEM medium. Cells were allowed 24 hours to attach and were then treated with BSO for an additional 18 hours (at a concentration of 200µM), after which cells were exposed to PAMAM G4 or G6 dendrimers (in DMEM F12 HAM, with 5%FBS, 45 IU/mL penicillin, 45 IU/mL streptomycin, 2mM L-glutamine and 200µM BSO) at various concentrations for the specified time points. Six replicates of each concentration were performed per plate and each plate was repeated in triplicate.

ThiolTracker™ Violet (TTV)

ThiolTracker™ Violet (TTV) is a GSH detection agent. Cells were plated as described above and a concentration gradient of BSO was applied. Cells were left for 18 hours at 37˚C in 5% CO_2 to allow for reduction of the amount of intracellular GSH. Cells were then washed twice with PBS, 100µL of TTV dye (at a final concentration of 20µM) were added to each well and the plates were allowed to incubate at 37˚C in 5% CO_2 for 30 minutes, after which the TTV solution was removed and replaced with PBS. The fluorescence of each well was then read using the SpectraMax M3 spectrometer with λ_{EX}= 404nm and λ_{EM}= 526nm. GSH values were calculated as compared to the unexposed control.

Viability assays

Alamar Blue and MTT assays were used to determine the changes in cell viability, after treatment with BSO as described above, as a result of exposure to both PAMAM G4 and G6

dendrimers. Both Alamar Blue and MTT were performed on the same plate. The PAMAM G4 concentrations used were: 0.16, 0.32, 0.65, 1.3, 2.6, 5.2, 7.8 and 10.4μM, while the PAMAM G6 concentrations were: 0.08, 0.16, 0.32, 0.65, 1.3, 2.6, 3.9 and 5.2μM. The lower initial value of the PAMAM G6 dendrimers was used due to their reported EC_{50} value being much lower than their G4 counterparts.[7,8,9] Dose dependent viability percentages were calculated at time points: 6, 12, 24, 48 and 72 hours. Percentage viability was calculated as compared to a control which had been exposed to 200μM BSO, but had no nanoparticle treatment; this was to ensure any changes were caused by the nanoparticle and were not the result of BSO treatment. A separate control where no BSO was present was also performed and showed there was little difference between cells with no BSO exposure and cells which were exposed to BSO (Supplementary Material, Figure: S1).

Alamar Blue (AB)

The Alamar Blue assay was made up from 10X stock solution in medium (DMEM F12 HAM, with no additional supplements). At the specified time point, the plates were removed from the incubator and the medium containing PAMAM dendrimer was removed, the cells were washed with 100μL PBS and then 100μL of DMEM F12 HAM(unsupplemented) containing Alamar Blue were added to each well. The plates were incubated for 3 hours at 37˚C in 5% CO_2 to allow for conversion of the dye. The fluorescence of each well was then read using the SpectraMax M3 spectrometer with λ_{EX}= 555nm and λ_{EM}= 585nm.

MTT (3-(4,5-dimethylthiazol-2-yl)-2,5-diphenyltetrazolium bromide)

A stock solution of MTT was made at a concentration of 0.5mg/mL. 500µL of this stock were added for every 10mL of medium (DMEM F12 HAM, with no additional supplements). At the specified time point, the plates were removed from the incubator and the medium containing PAMAM dendrimer was discarded, the cells were washed with 100µL PBS and then 100µL of DMEM (unsupplemented) containing MTT was added to each well. The plates were incubated for 3 hours at 37˚C in 5% CO_2 to allow for conversion of the dye. After 3 hours, any remaining dye was removed and each well was again washed with 100µL PBS, after which 100µL of DMSO was added and the plates were placed on a shaker for 10 minutes to allow for the dye to solubilise. The absorbance of each well was then read using the SpectraMax M3 spectrometer with λ_{ABS}=595nm.

Reactive Oxygen Species (ROS)

5-(and-6)-carboxy-2',7'-dichlorodihydrofluorescein diacetate (carboxy-H_2DCFDA) dye was used for the detection of ROS. The dye was made up to a final concentration of 10µM in sterile PBS. Before addition of PAMAM dendrimer, this dye was added to the cells and allowed to incubate for 1 hour, after which, the dye was removed, the cells were washed thrice with PBS and the medium containing PAMAM dendrimer was added. At the specified time points the fluorescence was read by the SpectraMax M3 spectrometer with λ_{EX}= 488nm and λ_{EM}= 535nm.

Confocal Laser Scanning Microscopy (CLSM)

Cells were plated onto MatTek 35mm glass bottom dishes at a concentration of 20,000 cells/dish in DMEM F12 HAM (supplemented with 10% FBS, 45 IU/mL penicillin, 45 IU/mL streptomycin and 2mM L-glutamine) and allowed to attach for 4 hours, at which point the

medium was removed and replaced with medium containing Celllight® Early Endosomes-RFP, BacMam 2.0 at a concentration of 20 particles per cell. Early endosome formation was tracked with the Celllight® Early Endosome – RFP kit, which transfects, into the cell, a version of Rab5a with a bound Red Fluorescent Protein. The cells were allowed to incubate (37˚C, 5% CO_2) for 16 hours to ensure transfection with the early endosome reagent. After this, the medium was removed and cells were washed twice with PBS. For cells being tested without BSO, medium was added for 18 hours (these samples are referred to as untreated cells/untreated controls in the text), while for cells being tested with BSO, medium containing 200μM BSO was added for 18 hours. Cells were again washed with PBS and carboxy-H_2DCFDA was added for 1 hour (10μM in 2mL PBS), after which cells were again washed twice with PBS. PAMAM dendrimers were added at a concentration of 3.21μM (G4) and 1μM (G6) and cells were allowed to incubate for 3 hours (G4) or 1 hour (G6) and were then washed twice with PBS and imaged with the Zeiss LSM 510 Confocal Laser Scanning Microscope. 100nm PSNP-NH_2 with attached Green Florescent Protein was used as a positive control to ensure the Celllight® Early Endosomes-RFP was functioning as expected; the results of this test are available in the supplementary material section, Figure S2. Negative controls were also performed with cells which were not exposed to any nanoparticles, and little to no fluorescence was noted (data not shown). For ROS monitoring, doses and time points noted above were chosen based on the maximum responses previously reported in literature.[8] All confocal images were analysed using ImageJ and co-localisation studies were performed using Manders split coefficients calculated with the JaCoP plugin for ImageJ.[42]

Data Analysis and Statistics

Data analysis was performed using SigmaPlot™ v10.0 and fluorescence was calculated based on the values of BSO controls (which were unexposed to nanoparticles, but had been treated with 200μM BSO for 18 hours).

"The cytotoxicity, GSH and ROS experiments were performed in 96-well microplates with six replicates per plate and each plate repeated three times. Therefore, data points shown represent the mean of 18 points, with error bars representing ± the standard deviation (as calculated by SigmaPlot™ v10.0). Confocal Images were taken on a Zeiss LSM 510 and processed using ImageJ software. Images were taken of eight cells/groups of cells and the images presented in the manuscript are representative of the sampled cell population."

Results

BSO treatment

While maximising the desired effect of the BSO on the cells, it is important that the viability of the cells is not affected. TTV showed a 40% reduction in intracellular levels of GSH for the HaCaT cells upon 200μM BSO exposure for 18 hours (adapted from the methods of: He *et al.* (*2003*)).[24] This dose and time point were found to have a minimal impact on cellular viability as measured by the AB and MTT assays (data available in Supplementary Material, Figure: S3). Higher concentrations were found to have an effect on cellular viability, although a more pronounced effect was observed by CLSM, where signs of cellular stress were noted (data not shown). Therefore 200μM BSO exposure was chosen as optimal.

PAMAM G4 dendrimers

CLSM was employed as a way to examine the effect of BSO treatment on the cellular uptake mechanisms and subsequent oxidative stress. Early endosome formation was tracked with the Celllight® Early Endosome – RFP kit and the formation of ROS was also tracked using the carboxy-H_2DCFDA dye. Fluorescently labelled PSNP-NH_2 of 100nm diameter were employed as positive controls, and the results for those are shown in the Supplementary Material: Figure S2.

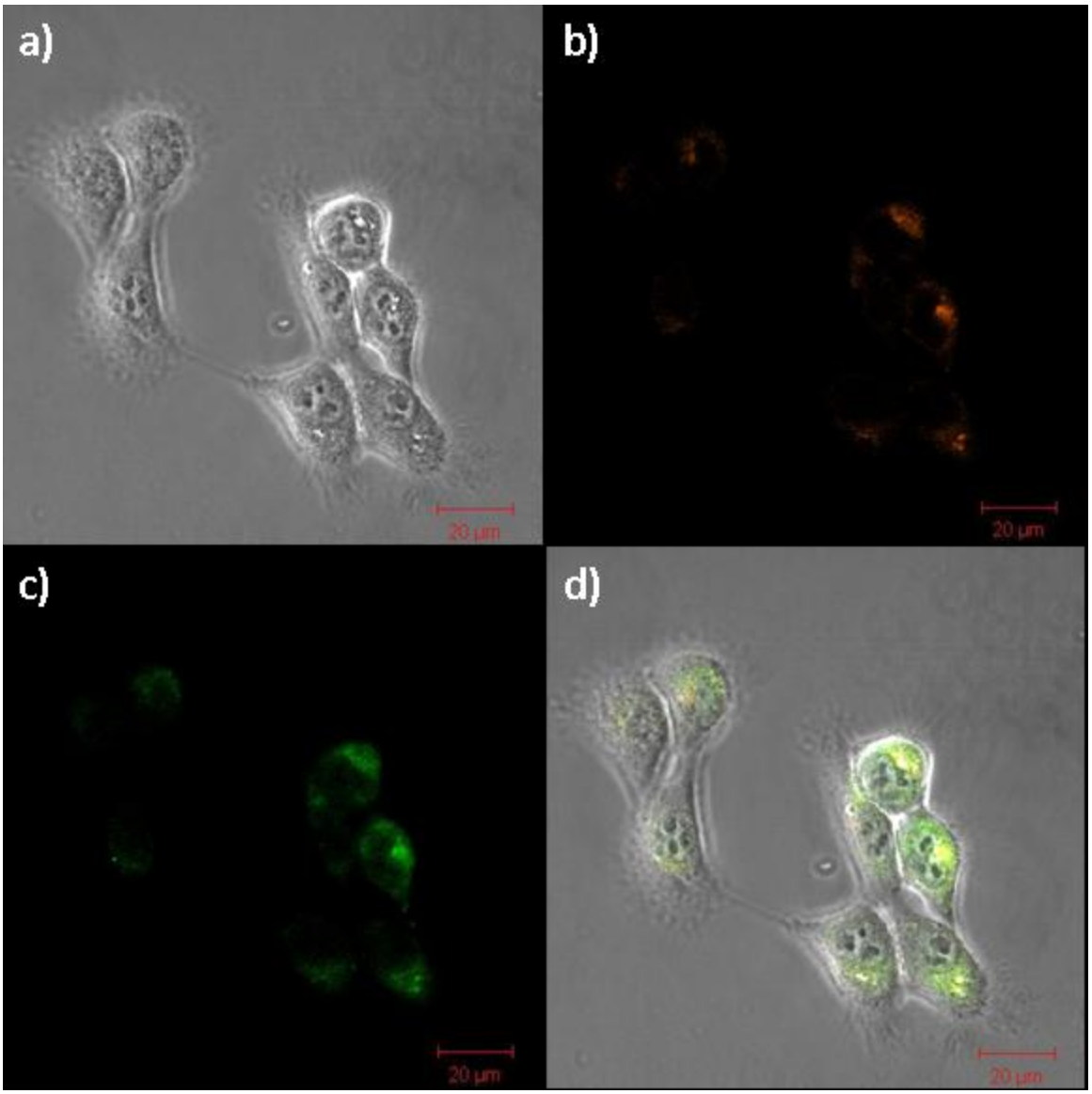

Figure 1: CLSM images of HaCaT (live) cells, upon exposure to 3.21µM PAMAM G4 dendrimer at 3 hours (no BSO is present in this sample). Image a) shows the bright field image of the cells, Image b) shows the fluorescence generated by the early endosomal red fluorescent protein, Image c) shows the fluorescence generated by the ROS (interacting with the carboxy-H_2DCFDA dye) and Image d) shows the overlay of images a-c, where yellow coloured areas indicate simultaneous endosomal and ROS activity.

Figure 1 shows the HaCaT cells following the reported paradigm of PAMAM G4 endocytosis and subsequent ROS generation at the endosomal sites.[6,7,8,9] Co-localisation (performed on the images in Figure 1) shows that 91(±3)% of the generated ROS occurs in the neighbourhood of endosomes, and that 71(±4)% of endosomal formation resulted in increases in ROS production (the other 30% of endosomal activity is most likely due to endocytosis which would be routinely done by the cell and would not involve the dendrimers and therefore not produce ROS).

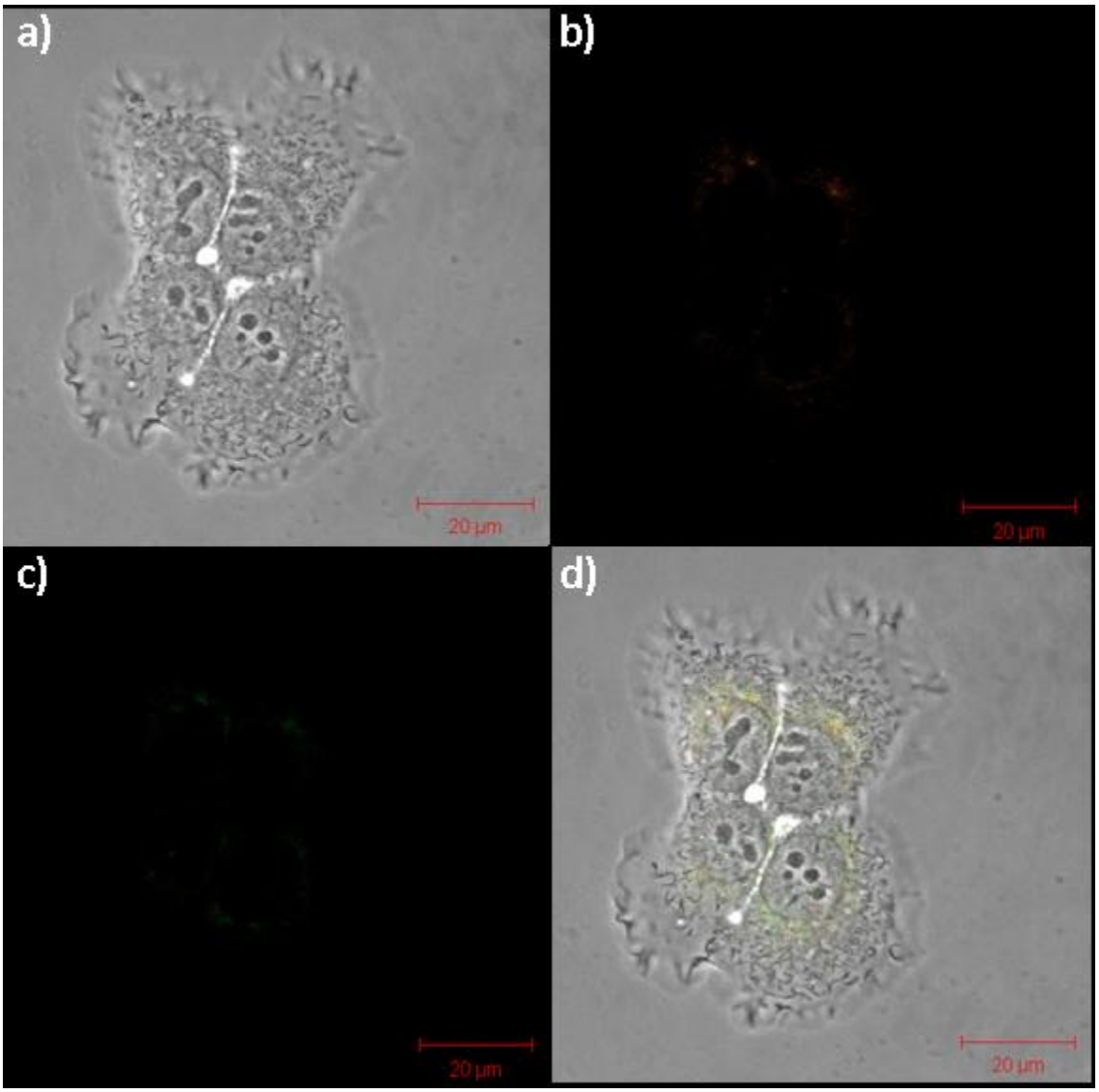

Figure 2: Confocal images of HaCaT (live) cells, upon exposure to 3.21μM PAMAM G4 dendrimer at 3 hours, with pre-treatment of BSO: 200μM for 18hours. Image a) shows the bright field image of the cells, Image b) shows the fluorescence generated by the early endosomal red fluorescent protein, Image c) shows the fluorescence generated by the ROS (interacting with the carboxy-H_2DCFDA dye) and Image d) shows the overlay of images a-c, where yellow coloured areas indicate simultaneous endosomal and ROS activity.

In contrast, Figure 2 shows HaCaT cells which have been treated with BSO for 18 hours prior to PAMAM G4 exposure (BSO was still present in the media upon exposure, to ensure conditions were consistent). In images (b) and (c), the intensity of the endosomal RFP and ROS dye have been significantly reduced. Again co-localisation analysis was performed (on images in Figure 2) and showed that 30(±6)% of the generated ROS was happening around the endosomes, and that 46(±14)% of endosomal formation resulted in increases in ROS production. Intensity analysis of the red fluorescent protein produced by endocytosis, on average, showed a reduction in intensity of 70(±3)% for cells treated with BSO.

Endosomal uptake was clearly reduced, although a decrease in the intensity of response of the ROS detection dye, carboxy-H_2DCFDA, was also noted, prompting a quantitative analysis of the ROS contents of the HaCaT cells: Figure 3.

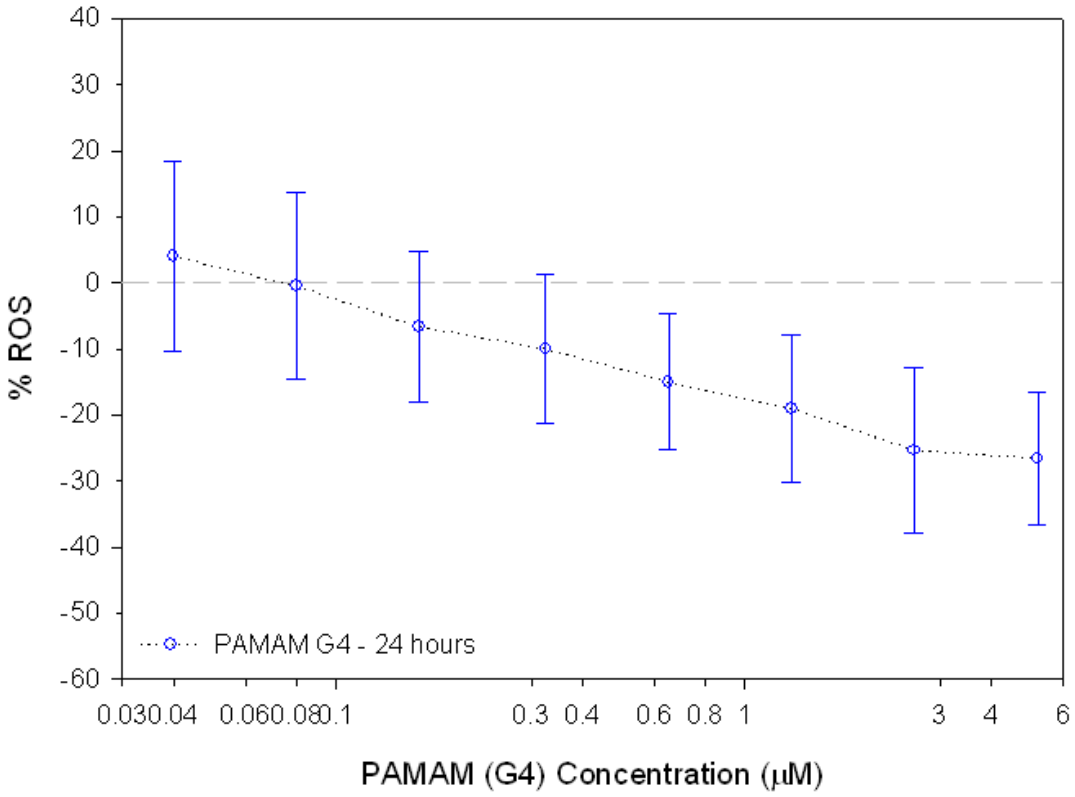

Figure 3: Dose dependant generation of ROS in HaCaT cells (shown for 24 hours for the PAMAM G4). ROS is compared to BSO control which was set to equal 0%. The X-axis is plotted logarithmically to allow for better visualisation of lower concentrations. Data points are the mean of 18 samples, with error bars showing (±) the standard deviation.

The analysis of ROS showed a net decrease at all doses tested; for clarity, only the dose dependence of the 24 hour test has been shown, the full data-set is available in the supplementary material section (Figure S4). Over the dose range tested, the ROS response followed a monotonically decreasing trend. This result, is again, in contrast with previous observations, in which ROS levels were seen to increase above control levels in a dose dependant fashion, upon G4 dendrimer exposure.[8]

To examine how these changes in both endocytosis and ROS production affected the viability of the cell AB and MTT assays were performed. HaCaT cells were exposed to 200µM BSO for 18 hours and subsequently exposed to varying concentrations of PAMAM G4 nanoparticles. Viability was measured at 6, 12, 24, 48 and 72 hours (Figure 4 (a) and (b)).

(a) (b)

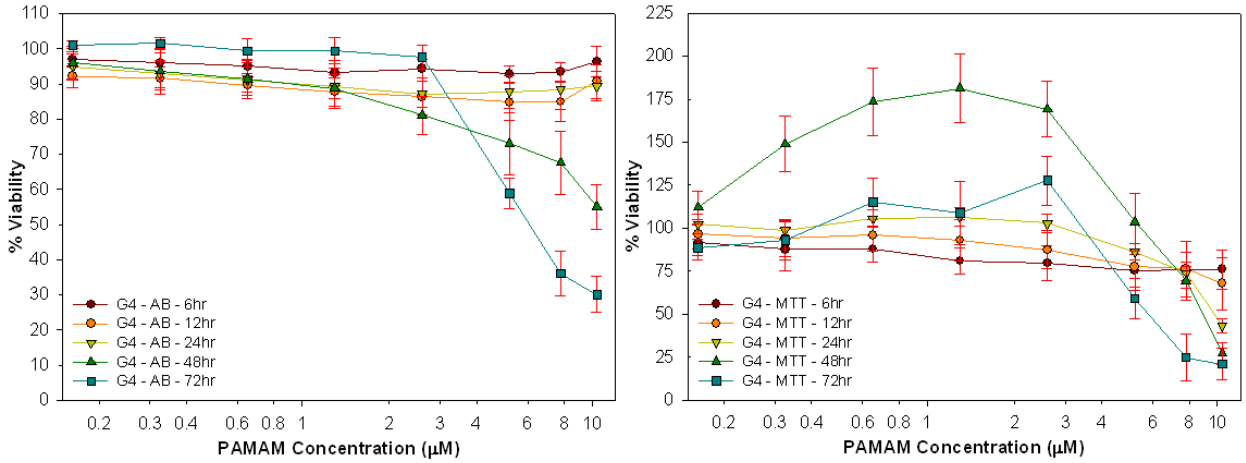

Figure 4: Alamar Blue (a) and MTT (b) dose dependant viability results for PAMAM G4 dendrimers in HaCaT cells after 6, 12, 24, 48 and 72 hours. Viability is calculated as the percentage of living cells as compared to BSO control. Data points are the mean of 18 samples, with error bars showing (±) the standard deviation.

The AB assay shows little or no toxicity of PAMAM G4 at time points 6, 12, and 24 hours, whereas the viability is reduced to 50% at 48 hours and 30% at 72 hours, for the higher dose exposures. In HaCaT cells which have not been treated with BSO, the EC_{50} obtained from AB is around 10µM at 24 hours,[7] whereas, in Figure 4, at the same time point, it is clear that there is no significant toxicity. The MTT results show a dramatically different dose dependent cytotoxicity profile for the BSO dosed cells compared to un-dosed.[7] At 6 hours exposure (Figure 4b), the

viability is seen to be reduced to around 80% over the entire dose range. However, at exposure times of 12, 24, 48 and 72 hours, increases in viability are seen for the low-medium dose range. The effect is particularly pronounced at the 48 hour time point, at which the recorded MTT response is ~175% of control, for an exposure dose of ~1μM. For doses of ~2.6μM and higher, the MTT assay response registers a decrease in viability, which is more pronounced in the longer time point exposures.

PAMAM G6 dendrimers

Analysis of uptake and ROS production was again carried out using CLSM (with the same method as the PAMAM G4) incorporating the carboxy-H_2DCFDA dye and Celllight® Early Endosome – RFP kit (Figure 5 and 6).

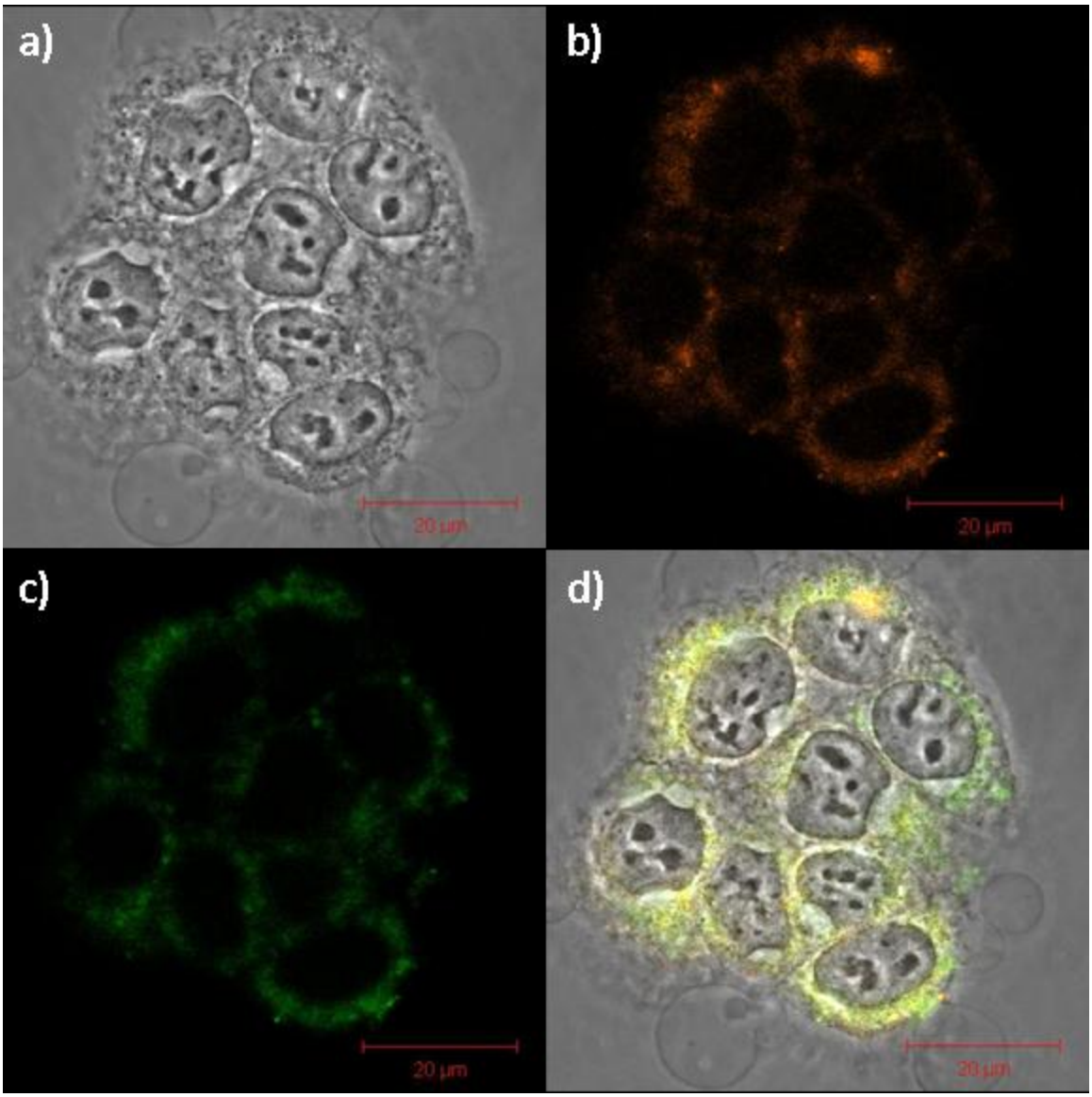

Figure 5: Confocal images of HaCaT (live) cells, upon exposure to 1µM PAMAM G6 dendrimer at 1 hour (no BSO is present in this sample). Image a) shows the bright field image of the cells, Image b) shows the fluorescence generated by the early endosomal red fluorescent protein, Image c) shows the fluorescence generated by the ROS (interacting with the carboxy-H_2DCFDA dye) and Image d) shows the overlay of images a-c, where yellow coloured areas indicate simultaneous endosomal and ROS activity.

In the absence of BSO, PAMAM G6 exposure, resulted in strong red fluorescence indicating a high level of endocytosis, complemented by strong green fluorescence indicating increased ROS production. Co-localisation analysis (of images in Figure 5) found that 75(±2)% of the generated ROS occurred in the region of the endosomes, and that 92(±1)% of endocytosis resulted in increases in ROS production. This strong level of co-localisation is indicative of the accepted paradigm of nanoparticle uptake by endocytosis, and ROS production at the site of endosomes.

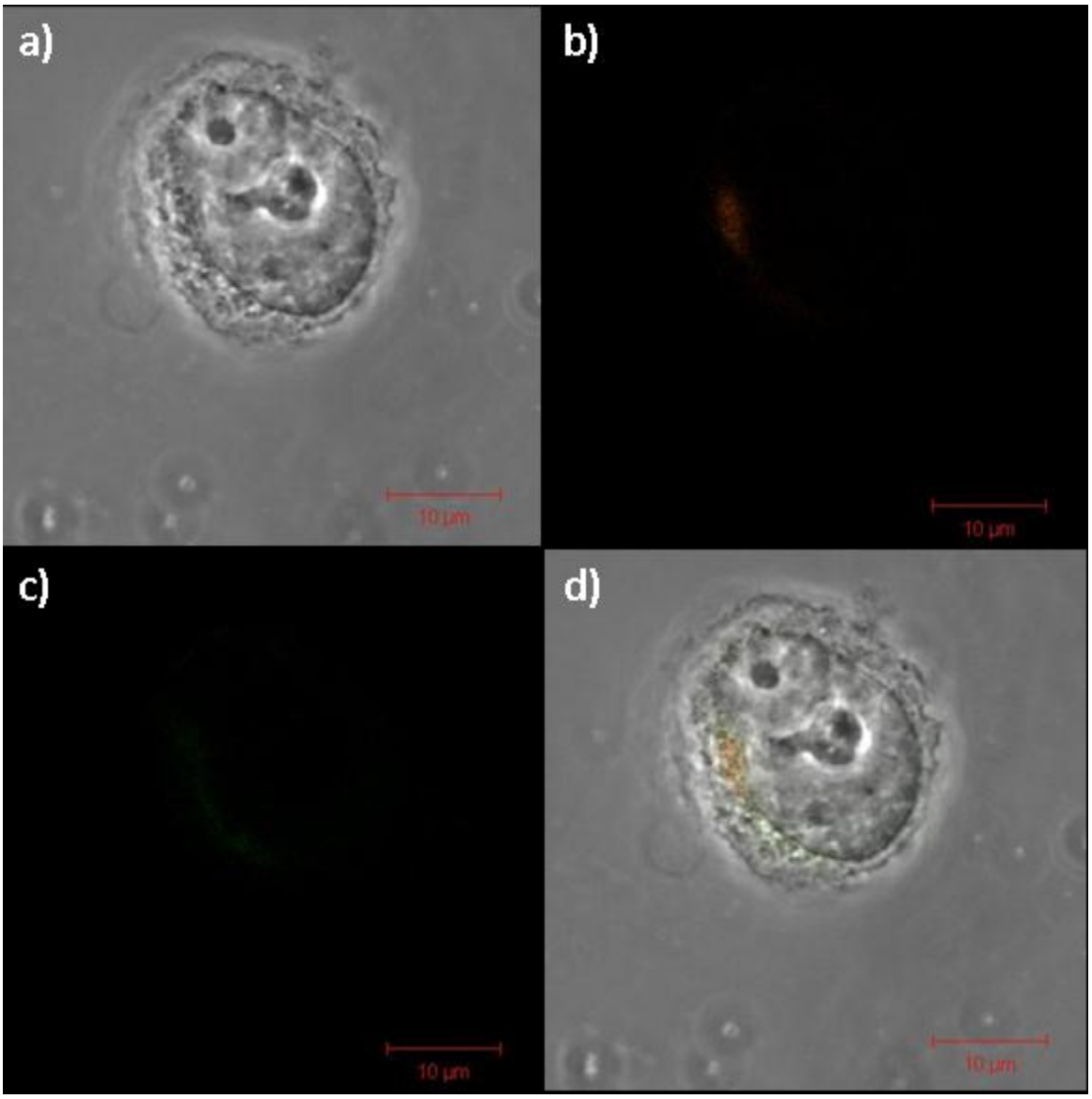

Figure 6: Confocal images of HaCaT (live) cells, upon exposure to 1μM PAMAM G6 dendrimer at 1 hour, with pre-treatment of BSO: 200μM. Image a) shows the bright field image of the cells, Image b) shows the fluorescence generated by the early endosomal red fluorescent protein, Image c) shows the fluorescence generated by the ROS (interacting with the carboxy-H_2DCFDA dye) and Image d) shows the overlay of images a-c, where yellow coloured areas indicate simultaneous endosomal and ROS activity.

In comparison to exposure of PAMAM G6 in cells without BSO treatment (untreated cells), there is a sparsity of endosomal activity and oxidative stress response in cells which had been pre-treated with BSO for 18 hours. Analysis (of the images in Figure 6) showed decreased levels of co-localisation between the ROS and endosomal formation: only 41(±18)% of ROS production was recorded in areas where endosomes had formed and 55(±10)% of endocytosis resulted in increases in ROS production. Intensity analysis of the red fluorescent protein produced by endocytosis, on average, showed a reduction in intensity of 61(±1)% for cells treated with BSO when compared to the untreated cells.

Again, in light of the reduced ROS response, quantitative analysis, using carboxy-H_2DCFDA was performed: Figure 7.

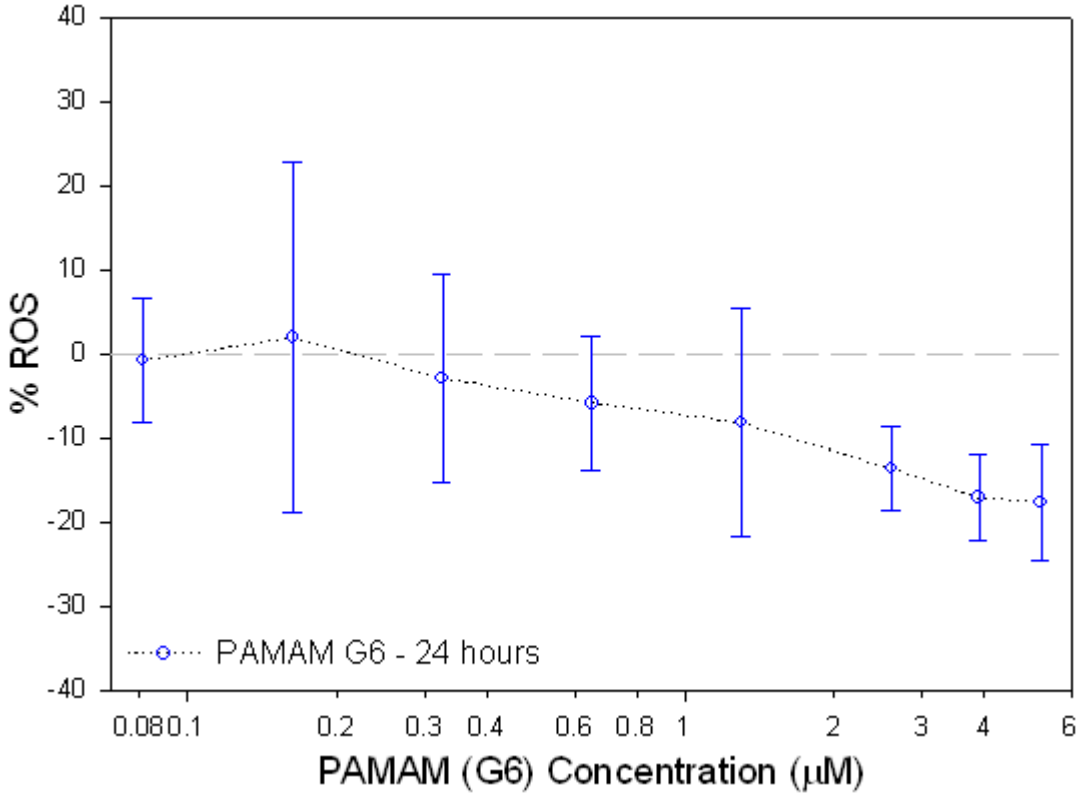

Figure 7: Dose dependant generation of ROS in HaCaT cells (shown at 24 hours for the PAMAM G6). ROS is compared to BSO control which was set to equal 0%. The X-axis is plotted logarithmically to allow for better visualisation of lower concentrations. Data points are the mean of 18 samples, with error bars showing (±) the standard deviation.

The dose response of the ROS generation shows similarities with the G4 in the overall progression of the response, pointing to a trend where increasing concentration leads to decreasing amounts of ROS, contrary to what has been observed in previous studies without BSO exposure.[8] As with the G4 analysis, for clarity, only one of the eight concentrations tested have been shown, the full data-set is available in the supplementary material section (Figure S5). At all doses tested, the ROS response followed the same trend as shown in Figure 7.

To analyse the effect this had on viability, AB and MTT assays were performed: Figure 8.

(a) (b)

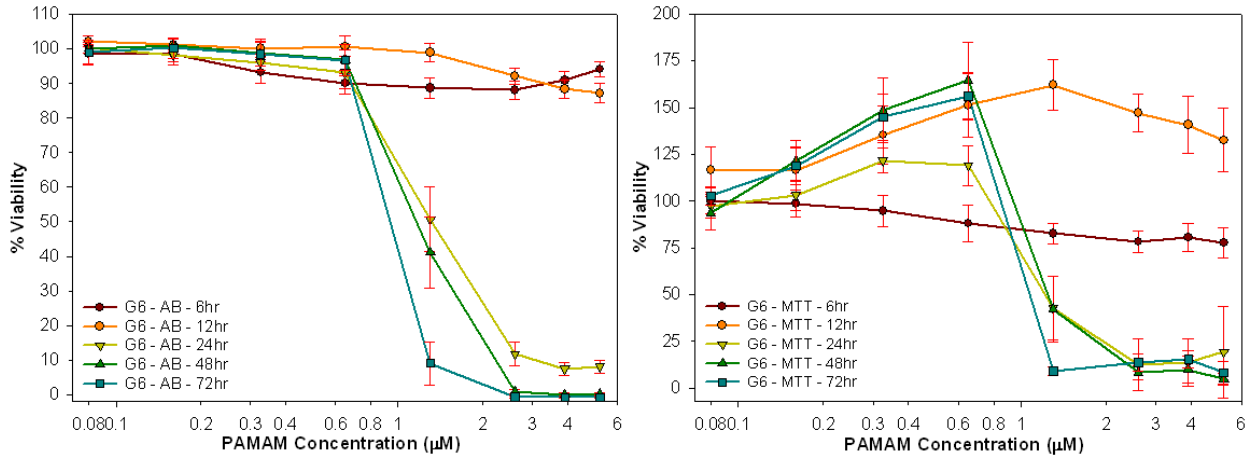

Figure 8: Alamar Blue (a) and MTT (b) dose dependant toxicity results for PAMAM G6 dendrimers in HaCaT cells after 6, 12, 24, 48 and 72 hours. Viability is calculated as the percentage of living cells as compared to a BSO control. The X-axis is plotted logarithmically to allow for better visualisation of lower doses. Data points are the mean of 18 samples, with error bars showing (±) the standard deviation.

The viability results of the PAMAM G6 dendrimers are similar to those observed in the G4 analysis. In Figure 8, for 6 and 12 hour exposure, little toxicity is recorded by AB, although the response is significantly stronger at the later time points. The previously reported EC_{50} obtained form the AB assay for PAMAM G6 dendrimers is in the range of 1μM-1.6μM at 24 hours,[8] which would appear to agree with the values obtained in this study. However, as was the case for PAMAM G4 exposure, the MTT assay registers increased percentage viability, compared to BSO control, for the intermediate doses, for all but the 6 hour exposure time point. A cytotoxic

response is elicited for doses greater than 1μM, for the 24, 48 and 72 hour time points and the response is consistent with the previously reported EC_{50} values of 0.92μM-1.13μM.[7]

PAMAM G4-G6 Comparative Analysis

PAMAM nanoparticle toxicity is a generation dependant process,[7,8,9] therefore, a comparison of the response of BSO treated cells to G4 and G6 dendrimer exposure was performed, to establish whether a similar generation dependence of the cellular responses is still evident.

The AB and MTT assays were compared for PAMAM G4 and G6 dendrimers, and the results are shown in Figures 9 (AB) and 10 (MTT). For both dendrimers, approximately equivalent concentration ranges were used, although, for the PAMAM G6 dendrimers, a slightly lower initial concentration was used due to the higher associated toxicity.[7,8,9,10]

a) b)

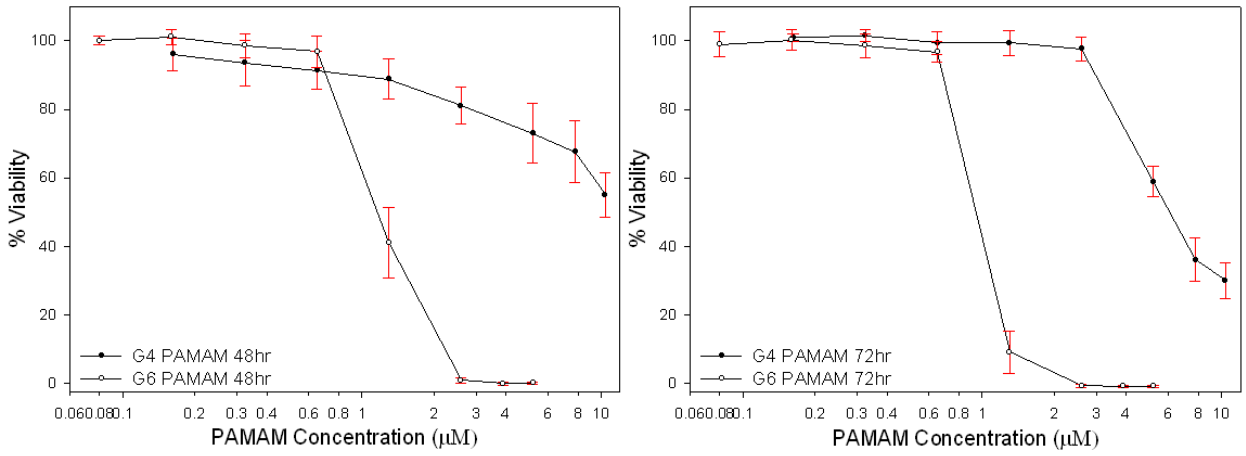

Figure 9: Alamar Blue (AB) dose dependant toxicity results comparing the PAMAM G4 and G6 dendrimers in HaCaT cells after 48 hours (a) and 72 hours (b). Viability is calculated as the percentage of living cells as compared to BSO control. The x-axis is plotted logarithmically to

allow for better visualisation of lower doses. Data points are the mean of 18 samples, with error bars showing (±) the standard deviation. 6, 12 and 24 hour graphs can be seen in the supplementary material section (Figure S6).

Little or no significant cytotoxicity was registered by the AB assay for either dendrimer at the 6 and 12 hour time points. At 24 hours, the higher toxicity associated with the G6 dendrimers becomes apparent, while the G4 still shows no significant change (Supplementary Material: Figure S6, c). At 48 hours (Figure 9(a)) the G4 dendrimers begin to elicit a significant toxic response and finally, at 72 hours (Figure 9(b)), the G4 toxic profile is beginning to match that of G6, although the reduction of viability is much higher for G6.

a) b)

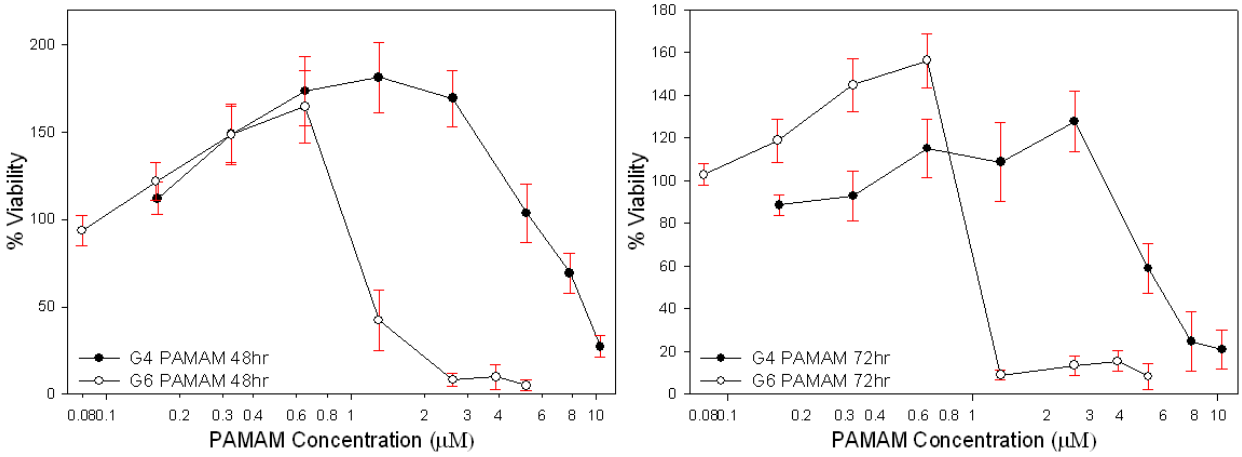

Figure 10: MTT dose dependant toxicity results comparing the PAMAM G4 and G6 dendrimers in HaCaT cells after 48 hours (a) and 72 hours (b). Viability is calculated as the percentage of living cells as compared to BSO control. The X-axis is plotted logarithmically to allow for better visualisation of lower doses. Data points are the mean of 18 samples, with error bars showing (±)

the standard deviation. 6, 12 and 24 hour graphs can be seen in the supplementary material section (Figure S7).

In the MTT, similar to AB response, no significant difference was seen in the 6 hour analysis for the two dendrimers, although differences become apparent at 12 hours (Supplementary Material: Figure S7, b), at which point the MTT response increases above that of controls for the G6 dendrimer. This increase in MTT response also occurs for the G4 dendrimers, although, it is not manifest until the later time point of 48 hours (Figure 10(a)). Similar to the AB response, cytotoxicity is registered by the MTT assay for both dendrimers beginning at 24 hours; however, the AB only reaches about 50% viability. At 48 and 72 hours a more complete toxic profile for both assays is seen and distinct generation dependence is observable, more consistent with that observed for untreated cells.[7]

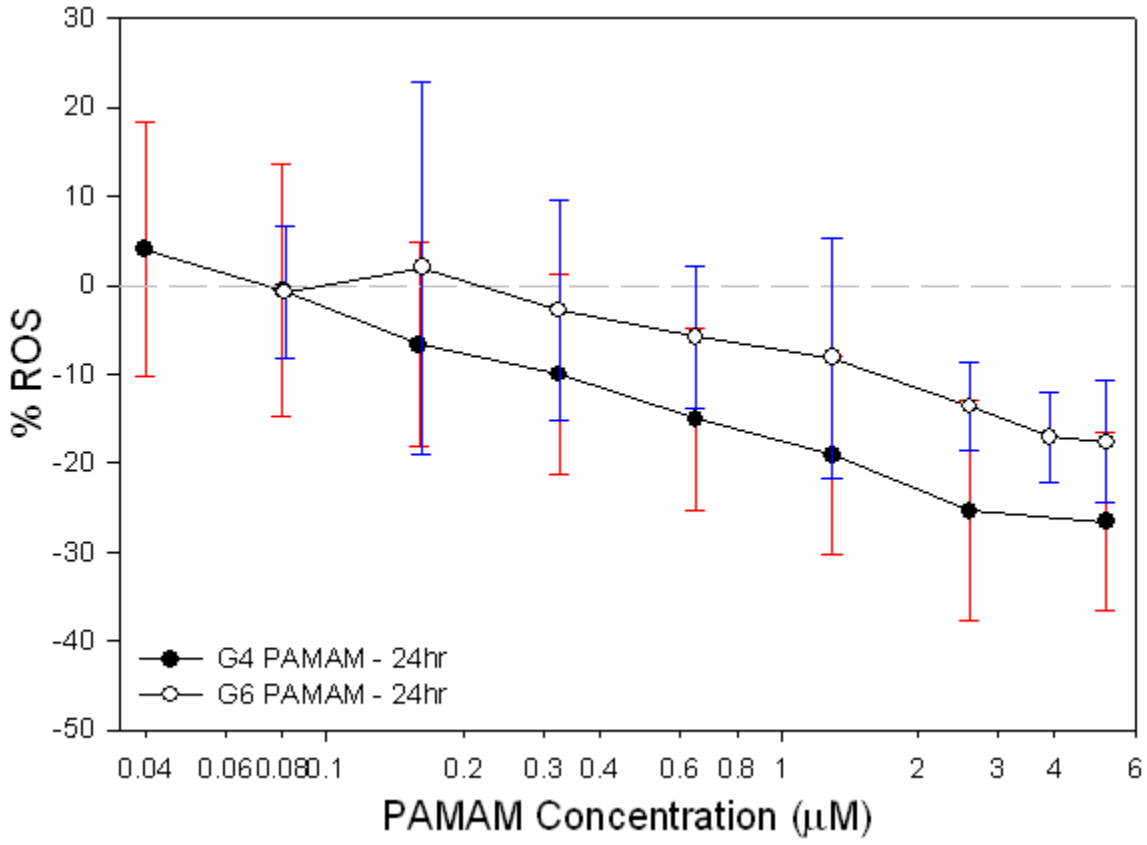

Figure 11: Dose dependant generation of ROS in HaCaT cells (shown at 24 hours for PAMAM G4 and G6). Data is compared to BSO control which was set to equal 0%. The X-axis is plotted logarithmically to allow for better visualisation of lower concentrations. Data points are the mean of 18 samples, with error bars showing (±) the standard deviation.

To further investigate any generation dependence, the dose response of the ROS was compared for the G4 and the G6 (Figure 11). It is notable that the generation dependence of the trends is reversed in Figure11 where G4 elicits a more pronounced reduction in ROS levels than G6.

Discussion

The confocal images of Figures: 1 and 2 (PAMAM G4) and Figures: 5 and 6 (PAMAM G6) show that, for cells treated with 200μM BSO for 18 hours prior to PAMAM exposure, the rate of endocytosis has been markedly reduced. This reduction in endocytosis is accompanied by a similar reduction in intracellular ROS and a dramatic change in the responses of the cytotoxic assays. Nevertheless, the observed reduction of intracellular ROS and cytotoxic responses are systematically dependent on dendrimer exposure time, dose and generation, consistent with the intracellular action of the dendritic nanoparticles.

The demonstrated mechanism of PAMAM dendrimer toxicity is one of endocytosis,[8,43,44] ROS production,[7,8,9,18] subsequent endosomolysis, whereby the nanoparticle bursts out of the endosome/lysosome into the cytosol,[19] and localisation in the mitochondria.[45] Mukherjee and Byrne (*2013*) identified two apoptotic pathways, the death-receptor pathway (extrinsic, Fas mediated FADD pathway[46]) and the mitochondrial pathway (intrinsic, TNF-α mediated FADD[47]).[10] The former is initiated by the earlier stage ROS generation in the region of the endosomes, while the latter is initiated by the localisation of the dendrimers in the mitochondria. It has been proposed that the early stage ROS production is due to the action of NADPH oxidase[6] (producing superoxide anions (O_2^-)[48]) and the v-ATPase proton pump (providing protons,[49] ultimately leading to production of H_2O_2[50] in and around the endosome. In cells treated with BSO, however, PAMAM dendrimers elicit a dramatically different cytotoxicity profile, as registered by the AB and MTT assays, compared to that of untreated cells.[7,8]

Studies by Khalid *et al.* (*2015*) of cellular uptake of PPI dendrimers have demonstrated that, although the larger generation PPI dendrimers are endocytosed and elicit similar responses to PAMAM equivalents in HaCaT cells, for smaller generation PPI dendrimers, uptake by passive diffusion occurs and, when the dendrimers enter the cell in this way, they were observed to act as antioxidants and elicit a significantly reduced cytotoxic effect.[18] BSO exposure has been shown to permeabilise the cell membrane,[28] and as a result, it is proposed that the PAMAM G4 and G6 dendrimers are able to circumvent the endocytotic process, are uptaken by passive diffusion, and, as PAMAM dendrimers are similar in structure to PPI dendrimers and have comparable surface chemistry, similarly behave as antioxidants in the cytosol, eliciting substantially reduced cytotoxic responses.

Alamar Blue is a non-specific assay and measures cellular viability based on the overall activity of the cytosolic environment.[51] The significant reduction, rather than expected increase, of toxicity as registered by this assay reflects the reduction in the endocytosis process (which initiates the Fas mediated FADD (death-receptor) apoptotic pathway), in favour of the passive diffusion of nanoparticles across the membrane, and consequent reduction in ROS generation in the region of endosomes. However, endocytosis is not fully eliminated for either generation, and therefore, the activation of the Fas mediated pathway, on a much reduced scale, would in part explain why the generation dependent response is still observed for the PAMAMs.

The MTT assay measures mitochondrial activity as an indicator of cellular viability[52,53,54] and, in the case of the studies described here, the mitochondria are implicated in at least two different processes and changes in MTT responses reflect the dose and generation dependence of these

processes at several time points. The first process is the loss of GSH from the cell, which has been shown to cause activation of mitochondrial signalling pathways and expression of genes associated with apoptosis, growth and differentiation.[33,38,39,40] This overall increase in mitochondrial activity (observed in the low dose regime), is seen as the initial increase in MTT values above controls, associated with dose and generation dependent decrease in ROS below controls, due to the antioxidant effect of the passively uptaken dendrimer nanoparticles.

The second effect gives rise to a sharp decrease in mitochondrial activity (observed in the higher dose regime); consistent with PAMAM dendrimer localisation and disruption of the mitochondria,[7,8] initiating the mitochondrial apoptotic pathway, leading to cell death in a dose dependant fashion, as observed for untreated cells.[7,8] This process may be accelerated via the opening of the mitochondrial membrane permeability transition pore.[30,31,32] Whether passively diffused into the cell, or released into the cytosol by endosomolysis after endocytosis, the result of free PAMAM dendrimers in the cytosol and subsequent localisation to the mitochondria should be equivalent, both resulting in disruption of the mitochondria, a second phase increase in ROS within the cell, subsequent decay in the mitochondrial membrane potential and finally the initiation of a cascade leading to apoptosis.[7,8,9,10] It should also be noted that in both cases the opening of the mitochondrial membrane transition pore occurs, either by the action of BSO,[30,31,32] or due to the release of the endosomal/lysosomal contents causing intracellular release of Ca^{2+}, leading to calcium dependant opening of the pore.[21] This would, in both cases, facilitate the entry of the dendrimer to the mitochondria. As a result, in the high dose regime, the observed toxic response of the BSO treated cells, as registered by the MTT assay, is not very different to that observed for untreated cells.

The passive diffusion of dendrimers across the cell membrane is a size dependant process[18] and, the generation dependence of the cellular responses to the two PAMAM dendrimer generations, G4 and G6, (Figures: 1, 2, 5 and 6), is consistent with a higher uptake rate for the G4 dendrimer than the G6. The greater reduction of intensity of Rab-5a-RFP compared to controls (with no BSO treatment), G4 dendrimers (70%) compared to G6 (60%), indicates a higher diffusion rate for G4 dendrimers, leaving fewer available for endocytosis. This further explains the higher rate of anti-oxidative activity exhibited by the G4 dendrimers when compared to G6 (Figure 11). Overall, it would appear that the membrane has become more permeable to an extent that favours passive uptake, although not completely eliminating active endocytosis.

Within the framework of Adverse Outcome Pathways (AOPs), recently endorsed by the OECD[55,56] as a method to simplify the representation of the mode of action of a toxicant or agonist, the generation of ROS can be considered the key Molecular Initiating Event (MIE) of the AOP, which ultimately leads to the AO of loss of cell viability. The treatment with BSO causes a depletion of GSH, which would lead to the expectation of much increased ROS levels after endocytosis. However, that was not observed and the result of the reduction of intrinsic GSH levels by BSO treatment was predominantly the increased permeability of the cell membrane, resulting in an increased rate of uptake of the PAMAM dendrimers by passive diffusion, making it a favoured uptake mechanism, more so for the smaller G4 dendrimer than the larger G6. The co-existence of the parallel uptake mechanisms increases the complexity of any model to describe the *in vitro* system, although it could prove a useful model to develop networks of AOPs, initiated by different MIEs. However, to fully examine the effect of reduction

of GSH in terms of decreased anti-oxidant activity alone, an assay which did not cause decrease of the permeabilisation of the cell membrane would be necessary.

Considering the potential for PAMAM dendrimers in nanomedical applications, it is important to note that, when diffused into the cell, the aminated surface chemistry of the dendrimers lend them antioxidant activity, similar to small molecular anti-oxidants, such as N-acetylcysteine (NAC) and NAC amide (NACA - a more bio-available version of NAC). NACA has been extensively studied as an antioxidant in the cell, due to its ability to diffuse across the membrane and the presence of a terminal proton donor group.[57,58] Interestingly, it has also been shown to completely reverse the damage caused to the cell by depletion of GSH.[59,60,61] NACA, due to this strong anti-oxidant ability, has been proposed in the treatment of several disorders and diseases, such as: HIV,[62] Alzheimer's and Parkinson's disease,[60,63] cataract formation,[59] retinal degeneration[64] and essentially any disease where ROS is identified as the potential MIE.[(See: 61 and references therein)] If PAMAM dendrimers are seen to act in a similar way, it may potentially allow for their use in a plethora of different nano-medical applications. As a strategy for drug release, endosomolysis can be extremely disruptive to the cell[20] and therefore, in the case of cationic nanoparticles for intracellular nanomedical applications, avoiding the process of endocytosis may be a valid strategy to pursue.[22] In terms of therapeutic applications, direct entry into the cytosol may be a more convenient route for drug or gene delivery.

Conclusions

Although PAMAM dendritic nanoparticles are known to elicit significant cytotoxic responses *in vitro*, the cellular response mechanisms can be notably altered by treatment of the cells with BSO. The treatment increases the cell membrane permeability, enabling uptake of the particles by passive diffusion, where after, they act as antioxidants in the cytosol, rather than producing oxidative stress in the region of endosomes. The ability to tune the cellular uptake mechanism allows direct entry into the cytosol and may have important implications for nanotoxicity as well as drug and gene delivery using nanovehicles.

Acknowledgements

The authors would like to thank Dr. Alan Casey and Esen Efeoglu for their contributions in the capturing and processing of the confocal images for this manuscript.

Funding Sources

Irish Government's Programme for Research in Third Level Institutions, Cycle 4, National Development Plan 2007-2013, supported by the European Union Structural Fund. M Maher is funded through the DIT Fiosraigh President's Award for Research Excellence 2010

Declaration of interest

The authors declare no conflict of interest related to the work presented in this manuscript.

References

1: Eichman, J.D., Bielinska, A.U., Kukowska-Latallo, J.F. and Baker, J.R.Jr. (2000) The use of PAMAM dendrimers in the efficient transfer of genetic material into cells. *J. Pharm. Sci. Technol. 3(7):* 233-245.

2: Duncan, R. and Izzo, L. (2005) Dendrimer biocompatibility and toxicity. *Adv. Drug. Deliv. Rev. 57(15):* 2215– 2237.

3: De Jong, W. H. and Borm, P.J.A. (2008) Drug delivery and nanoparticles: Applications and hazards. *Int. J. Nanomedicine. 3(2):* 133–149.

4: Nel, A., Xia, T., Mädler, L. and Li, N. (2006) Toxic potential of materials at the nanolevel. *Science. 311(5761):* 622-627.

5: Jain, K.K., Kesharwani, P., Gupta, U. and Jain, N.K. (2010) Dendrimer toxicity: Let's meet the challenge. *Int. J. Pharm. 394(1-2):* 122–142.

6: Xia, T., Kovochich, M., Brant, J., Hotze, M., Sempf, J., Oberley, T., Sioutas, C., Yeh, J.I., Wiesner, M.R. and Nel, A.E. (2006) Comparison of the Abilities of Ambient and Manufactured Nanoparticles to Induce Cellular Toxicity According to an Oxidative Stress Paradigm. *Nano Lett. 6(8):* 1794-1807.

7: Mukherjee, S.P., Davoren, M. and Byrne, H.J. (2010) *In vitro* mammalian cytotoxicological study of PAMAM dendrimers - towards quantitative structure activity relationships. *Toxicol. in Vitro, 24(1):* 169-177.

8: Mukherjee, S.P., Lyng, F.M., Garcia, A., Davoren, M. and Byrne H.J. (2010) Mechanistic studies of *in vitro* cytotoxicity of Poly(amidoamine) dendrimers in mammalian cells. *Toxicol. Appl. Pharmacol. 248(3):* 259–268.

9: Naha, P.C., Davoren, M., Lyng, F.M. and Byrne, H.J. (2010) Reactive Oxygen Species (ROS) induced cytokine production and cytotoxicity of PAMAM dendrimers in J774A.1 cells. *Toxicol. Appl. Pharmacol. 246(1-2):* 91-99

10: Mukherjee S.P. and Byrne, H.J. (2013) Polyamidoamine Dendrimer Nanoparticle Cytotoxicity, Oxidative Stress, Caspase Activation and Infammatory Response: Experimental Observation and Numerical Simulation. *Nanomed. Nanotech. Biol. Med. 9(2):* 202-211.

11: Anguissola, S., Garry, D., Salvati, A., O'Brien, P.J. and Dawson, K.A. (2014) High Content Analysis Provides Mechanistic Insights on the Pathways of Toxicity Induced by Amine-Modified Polystyrene Nanoparticles. *PLoS ONE*, 9(9): e108025. doi:10.1371/journal.pone.0108025

12: Paget, V., Dekali, S., Kortulewski, T., Grall, R., Gamez, C., Blazy, K., Aguerre-Chariol, O., Chevillard, S., Braun, A., Rat, P and Lacroix, G. (2015) Specific Uptake and Genotoxicity

643 Induced by Polystyrene Nanobeads with Distinct Surface Chemistry on Human Lung Epithelial
644 Cells and Macrophages. *PLoS ONE, 10(4):* e0123297. doi:10.1371/journal.pone.0123297
645
646 13: Lunov, O., Syrovets, T., Loos, C., Beil, J., Delacher, M., Tron, K., Nienhaus, G.U.,
647 Musyanovych, A., Mailänder, V., Landfester, K. and Simmet, T. (2011) Differential Uptake of
648 Functionalized Polystyrene Nanoparticles by Human Macrophages and a Monocytic Cell Line.
649 *ACS Nano. 5(3):* 1657-1669.
650
651 14: Nabeshi, H., Yoshikawa, T., Matsuyama, K., Nakazato, Y., Tochigi, S., Kondoh, S., Hirai,
652 T., Akase, T.,Nagano, K., Abe, Y., Yoshioka, Y., Kamada, H., Itoh, N., Tsunoda, S. and
653 Tsutsumi, Y. (2011) Amorphous nanosilica induce endocytosis dependent ROS generation and
654 DNA damage in human keratinocytes. *Part. Fibre Toxicol. 8(1):* 10 pages.
655
656 15: Mozdzan, M., Szemraj, J., Rysz, J., Stolarek, R.A. and Nowak, D. (2006) Anti-oxidant
657 activity of spermine and spermidine re-evaluated with oxidising system involving iron and
658 copper ions. *Int. J. Biochem. Cell Biol. 38(1):* 69-81.
659
660 16: Lotito, S.B. and Frei, B. (2004) Relevance of apple polyphenols as antioxidants in human
661 plasma: contrasting in vitro and in vivo effects. *Free Radic. Biol. Med. 36(2):* 201-211.
662
663 17: Hipkiss AR. (2009) Carnosine and its possible roles in nutrition and health. *Adv. Food Nutr.*
664 *Res. 57(-):* 87-154.
665

18: Khalid, H., Mukherjee, S.P., O'Neill, L. and Byrne, H.J. (2015) Structural dependence of the *In vitro* cytotoxicity, oxidative stress and uptake mechanisms of Poly(propylene imine) dendritic nanoparticles. *J. Appl. Toxicol*. (in press - Accepted: October 2015)

19: Watson, P., Jones, A.T. and Stephens, D.J. (2005) Intracellular trafficking pathways and drug delivery: fluorescence imaging of living and fixed cells. *Adv. Drug Deliver. Rev. 57(1):* 43-61.

20: Mukherjee, S.P. (2012) Towards Structure Activity Relationships for *in vitro* Toxicity of Polyamidoamine Dendritic Nanoparticles. *Thesis (PhD)*, Dublin Institute of Technology: 2012. Dublin: DIT.

21: Xia. T., Kovochich, M., Liong, M., Mädler, L., Gilbert, B., Shi, H., Yeh, J.I., Zink, J.I. and Nel, A.E. (2008) Comparison of the mechanism of toxicity of zinc oxide and cerium oxide nanoparticles based on dissolution and oxidative stress properties. *ACS Nano. 2(10):* 2121-2134.

22: Guarnieri, D., Sabella, S., Muscetti, O., Belli, V., Malvindi, M.A., Fusco, S., De Luca, E., Pompa, P.P. and Netti, P.A. (2014) Transport across the cell-membrane dictates nanoparticle fate and toxicity: a new paradigm in nanotoxicology. *Nanoscale. 6(17):* 10264-10273.

23: Girard, P-M., Graindorge, D., Smirnova, V., Rigolet, P., Francesconi, S., Scanlon, S. and Sage, E. (2013) Oxidative Stress in Mammalian Cells Impinges on the Cysteines Redox State of Human XRCC3 Protein and on Its Cellular Localization. *PLoS ONE,* DOI: 10.1371/journal.pone.0075751

24: He, Y-Y., Huang, J-L., Ramirez, D.C. and Chignell, C.F. (2003) Role of Reduced Glutathione Efflux in Apoptosis of Immortalized Human Keratinocytes Induced by UVA. *J. Biol. Chem. 278(10):* 8058–8064.

25: Madesh, M., Benard, O. and Balasubramanian, K.A. (1998) Glutathione modulates lipid composition of human colon derived HT-29 cells. *Int. J. Biochem. Cell Biol. 30(12):* 1345-1352.

26: Tobi, S.E., Paul, N. and McMillan T.J. (2000) Glutathione modulates the level of free radicals produced in UVA-irradiated cells. *J. Photochem. Photobiol. B. 57(2-3):* 102–112.

27: Li, X.Y., Donaldson, K., Rahman, I. and Mac Nee, W. (1994) An investigation of the role of glutathione in increased epithelial permeability induced by cigarette smoke *in vivo* and *in vitro*. *Am. J. Respir. Crit. Care Med. 149(6):* 1518-1525.

28: Zaman, G.J., Lankelma, J., van Tellingen, O., Beijnen, J., Dekker, H., Paulusma, C., Oude Elferink, R.P., Baas, F. and Borst, P. (1995) Role of glutathione in the export of compounds from cells by the multidrug-resistance-associated protein. *Proc. Natl. Acad. Sci. USA. 92(17):* 7690-7694.

29: Griffith, O.W. (1982) Mechanism of Action, Metabolism, and Toxicity of Buthionine Sulfoximine and Its Higher Homologs, Potent Inhibitors of Glutathione Synthesis. *J. Biol. Chem. 257(22):* 13704-13712.

712

713 30: Armstrong, J.S. and Jones, D.P. (2002) Glutathione depletion enforces the mitochondrial
714 permeability transition and causes cell death in Bcl-2 overexpressing HL60 cells. *FASEB J.*
715 *16(10):* 1263-1265.

716

717 31: Chernyak, B.V. and Bernardi, P. (1996) The mitochondrial permeability transition pore is
718 modulated by oxidative agents through both pyridine nucleotides and glutathione at two separate
719 sites. *Eur. J. Biochem. 238(3):* 623–630.

720

721 32: Reed, D.J. and Savage, M.K. (1995) Influence of metabolic inhibitors on mitochondrial
722 permeability transition and glutathione status. *Biochim. Biophys. Acta. 1271(1):* 43–50.

723

724 33: Circu, M.L. and Aw, T.Y. (2008) Glutathione and apoptosis. *Free Radic. Res. 42(8):* 689–
725 706.

726

727 34: Lash, L.H. (2006) Mitochondrial Glutathione Transport: Physiological, Pathological and
728 Toxicological Implications. *Chem. Biol. Interact. 163(1-2):* 54–67.

729

730 35: Beatrice, M.C., Stiers, D.L. and Pfeiffer, D.R. (1984) The role of glutathione in the retention
731 of Ca^{2+} by liver mitochondria. *J. Biol. Chem. 259(2):* 1279–1287.

732

733 36: Lotscher, H.R., Winterhalter, K.H., Carafoli, E. and Richter, C. (1979) Hydroperoxides can
734 modulate the redox state of pyridine nucleotides and the calcium balance in rat liver
735 mitochondria. *Proc. Natl. Acad. Sci. USA. 76(9):* 4340–4344.
736
737 37: Olafsdottir, K., Pascoe, G.A. and Reed, D.J. (1988) Mitochondrial glutathione status during
738 Ca2+ ionophore-induced injury to isolated hepatocytes. *Arch. Biochem. Biophys. 263(1):* 226–
739 235.
740
741 38: Davis, W.Jr., Ronai, Z. and Tew, K.D. (2001) Cellular thiols and reactive oxygen species in
742 drug-induced apoptosis. *J. Pharmacol. Exp. Ther. 296(1):* 1–6.
743
744 39: Petit, P.X., Susin, S.A., Zamzami, N., Mignotte, B. and Kroemer, G. (1996) Mitochondria
745 and programmed cell death: Back to the future. *FEBS Lett. 396(1):* 7–13.
746
747 40: Skulachev, V.P. (1996) Why are mitochondria involved in apoptosis? Permeability transition
748 pores and apoptosis as selective mechanisms to eliminate superoxide-producing mitochondria
749 and cells. *FEBS Lett. 397(1):* 7–10.
750
751 41: Maher, M.A., Naha, P.C., Mukerjee, S.P. and Byrne, H.J. (2014) Numerical simulations of in
752 vitro nanoparticle toxicity – the case of Poly(amido amine) dendrimers. *Toxicol. In Vitro. 28(8):*
753 1449-1460.
754

42: Zinchuk, V. and Zinchuk, O. (2008) Quantitative colocalization analysis of confocal fluorescence microscopy images. *Curr. Protoc. Cell Biol. Ch.4(Unit 4.19),* 1-16.

43: Kitchens, K.M., Foraker, A.B., Kolhatkar, R.B., Swaan, P.W., Ghandehari, H. (2007) Endocytosis and interaction of poly (Amidoamine) dendrimers with Caco-2 cells. *Pharmaceut. Res. 24(11):* 2138–2145.

44: Hong, S., Bielinska, A.U., Mecke, A., Keszler, B., Beals, J.L., Shi, X., Balogh, L., Orr, B.G., Baker, J.R.Jr and Banaszak Holl, M.M. (2004) Interaction of poly(amidoamine) dendrimers with supported lipid bilayers and cells: hole formation and the relation to transport. *Bioconjugate Chem. 15(4):* 774–782.

45: Lee, J.H., Cha, K.E., Kim, M.S., Hong, H.W., Chung, D.J., Ryu, G. and Myung, H. (2009) Nanosized polyamidoamine (PAMAM) dendrimer-induced apoptosis mediated by mitochondrial dysfunction. *Toxicol. Lett. 190(2):* 202–207.

46: Wajant, H. (2002) The Fas signaling pathway: more than a paradigm. *Science 296(5573):*1635-1636.

47: Desagher, S. and Martinou, J.C. (2000) Mitochondria as the central control point of apoptosis. *Trends Cell Biol. 10(9):* 369-377.

48: Shuvaev, V.V., Han, J., Yu, K.J., Huang, S., Hawkins, B.J., Madesh, M., Nakada, M. and Muzykantov, V.R. (2011) PECAM-targeted delivery of SOD inhibits endothelial inflammatory response. *FASEB J. 25(1):* 348-357.

49: Nel, A.E., Mädler, L., Velegol, D., Xia, T., Hoek, E.M.V., Somasundaran, P., Klaessig, F., Castranova, V. and Thompson, M. (2009) Understanding biophysicochemical interactions at the nano–bio interface. *Nature Materials. 8(7):* 543 – 557.

50: Babior, B.M., Lambeth, J.D. and Nauseef, W. (2002) The neutrophil NADPH oxidase. *Arch. Biochem. Biophys. 397(2):* 342–344.

51: O'Brien, J., Wilson, I., Orton, T. and Pognan, F. (2000) Investigation of the Alamar Blue (resazurin) fluorescent dye for the assessment of mammalian cell cytotoxicity. *Eur. J. Biochem. 267(17):* 5421-5426.

52: Mosmann, T. (1983) Rapid colorimetric assay for cellular growth and survival: Application to proliferation and cytotoxicity assays. *J. Immunol. Methods. 65(1):* 55-63.

53: Denizot, F. and Lang, R. (1986) Rapid colorimetric assay for cell growth and survival: Modifications to the tetrazolium dye procedure giving improved sensitivity and reliability. *J. Immunol. Methods. 89(2):* 271-277.

54: Hansen, M.B., Nielsen, S.E. and Berg, K. (1989) Re-examination and further development of a precise and rapid dye method for measuring cell growth/cell kill. *J. Immunol. Methods. 119(2):* 203-210.

55: Organisation for Economic Co-Operation and Development (OECD): Guidance Document on the Validation of (Quantative) Structure Activity Relationships [(Q)SAR] Models, *OECD, ENV/JM/MONO(2007)2*, 2007.

56: Organisation for Economic Co-Operation and Development (OECD): Guidance Document On Developing and Assessing Adverse Outcome Pathways, *OECD, ENV/JM/MONO(2013)6*, 2013.

57: Price, T.O., Uras, F., Banks, W.A. and Ercal, N. (2006) A novel antioxidant N-acetylcysteine amide prevents gp120- and Tat-induced oxidative stress in brain endothelial cells. *Exp. Neurol. 201(1):* 193–202.

58: Grinberg, L., Fibach, E., Amer, J. and Atlas, D. (2005) N-acetylcysteine amide, a novel cell permeating thiol, restores cellular glutathione and protects human red blood cells from oxidative stress. *Free Radic. Biol. Med. 38(1):* 136–145.

59: Carey, J.W., Pinarci, E.Y., Penugonda, S., Karacal, H. and Ercal, N. (2011) *In vivo* inhibition of l-buthionine-(S,R)-sulfoximine-induced cataracts by a novel antioxidant, N-acetylcysteine amide. *Free Radic. Biol. Med*. *50(6):* 722–729.

60: Penugonda, S., Mare, S., Goldstein, G., Banks, W.A. and Ercal, N. (2005) Effects of N-acetylcysteine amide (NACA), a novel thiol antioxidant against glutamate-induced cytotoxicity in neuronal cell line PC12. *Brain Research. 1056(2):* 132–138.

61: Sunitha, K., Hemshekhar, M., Thushara, R.M., Santhosh, M.S., Yariswamy, M., Kemparaju, K. and Girish, K.S. (2013) N-Acetylcysteine amide: a derivative to fulfill the promises of N-Acetylcysteine. *Free Radic. Res. 47(5):* 357-367.

62: Banerjee, A., Zhang, X., Manda, K.R., Banks, W.A. and Ercal, N. (2010) HIV proteins (gp120 and Tat) and methamphetamine in oxidative stress-induced damage in the brain: potential role of the thiol antioxidant N-acetylcysteine amide. *Free Radic. Biol. Med. 48(10):* 1388-1398.

63: Lee, K.S., Kim, S.R., Park, H.S., Park, S.J., Min, K.H., Lee, K.Y., Choe, Y.H., Hong, S.H., Han, H.J., Lee, Y.R., Kim, J.S., Atlas, D. and Lee, Y.C. (2007) A novel thiol compound, N-acetylcysteine amide, attenuates allergic airway disease by regulating activation of NF-kappaB and hypoxia-inducible factor-1alpha. *Exp. Mol. Med. 39(6):* 756-768.

64: Schimel, A.M., Abraham, L., Cox, D., Sene, A., Kraus, C., Dace, D.S., Ercal, N. and Apte, R.S. (2011) N-acetylcysteine amide (NACA) prevents retinal degeneration by up-regulating reduced glutathione production and reversing lipid peroxidation. *Am. J. Pathol. 178(5):* 2032-2043.